This article was downloaded by: [Institute Of Atmospheric Physics]
On: 09 December 2014, At: 15:14
Publisher: Taylor & Francis
Informa Ltd Registered in England and Wales Registered Number: 1072954 Registered office: Mortimer House, 37-41 Mortimer Street, London W1T 3JH, UK

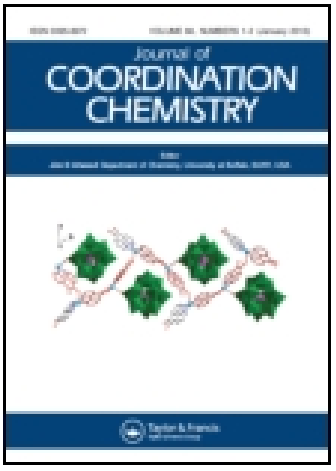

CrossMark
Click for updates

Journal of Coordination Chemistry
Publication details, including instructions for authors and subscription information:
http://www.tandfonline.com/loi/gcoo20

Synthesis and structure of Zn(II) and Cu(II) complexes derived from 2-(aminomethyl)benzimidazole and glycine

Martha Falcón-León[a], Hugo Tlahuext[b], Víctor Lechuga-Islas[a], Margarita Tlahuextl[a], Francisco J. Martínez-Martínez[c], Herbert Höpfl[b] & Antonio R. Tapia-Benavides[a]

[a] Centro de Investigaciones Químicas, Universidad Autónoma del Estado de Hidalgo, Mineral de la Reforma, Mexico

[b] Centro de Investigaciones Químicas, Universidad Autónoma del Estado de Morelos, Cuernavaca, Mexico

[c] Facultad de Ciencias Químicas, Universidad de Colima, Colima, Mexico

Accepted author version posted online: 05 Jun 2014.Published online: 01 Jul 2014.

To cite this article: Martha Falcón-León, Hugo Tlahuext, Víctor Lechuga-Islas, Margarita Tlahuextl, Francisco J. Martínez-Martínez, Herbert Höpfl & Antonio R. Tapia-Benavides (2014) Synthesis and structure of Zn(II) and Cu(II) complexes derived from 2-(aminomethyl)benzimidazole and glycine, Journal of Coordination Chemistry, 67:11, 1873-1887, DOI: 10.1080/00958972.2014.930139

To link to this article: http://dx.doi.org/10.1080/00958972.2014.930139

PLEASE SCROLL DOWN FOR ARTICLE

Taylor & Francis makes every effort to ensure the accuracy of all the information (the "Content") contained in the publications on our platform. However, Taylor & Francis, our agents, and our licensors make no representations or warranties whatsoever as to the accuracy, completeness, or suitability for any purpose of the Content. Any opinions and views expressed in this publication are the opinions and views of the authors, and are not the views of or endorsed by Taylor & Francis. The accuracy of the Content should not be relied upon and should be independently verified with primary sources of information. Taylor and Francis shall not be liable for any losses, actions, claims, proceedings, demands, costs, expenses, damages, and other liabilities whatsoever or howsoever caused arising directly or indirectly in connection with, in relation to or arising out of the use of the Content.

This article may be used for research, teaching, and private study purposes. Any substantial or systematic reproduction, redistribution, reselling, loan, sub-licensing, systematic supply, or distribution in any form to anyone is expressly forbidden. Terms & Conditions of access and use can be found at http://www.tandfonline.com/page/terms-and-conditions

Downloaded by [Institute Of Atmospheric Physics] at 15:14 09 December 2014

Journal of Coordination Chemistry, 2014
Vol. 67, No. 11, 1873–1887, http://dx.doi.org/10.1080/00958972.2014.930139

Taylor & Francis
Taylor & Francis Group

Downloaded by [Institute Of Atmospheric Physics] at 15:14 09 December 2014

Synthesis and structure of Zn(II) and Cu(II) complexes derived from 2-(aminomethyl)benzimidazole and glycine

MARTHA FALCÓN-LEÓN†, HUGO TLAHUEXT*‡, VÍCTOR LECHUGA-ISLAS†, MARGARITA TLAHUEXTL†, FRANCISCO J. MARTÍNEZ-MARTÍNEZ§, HERBERT HÖPFL‡ and ANTONIO R. TAPIA-BENAVIDES*†

†Centro de Investigaciones Químicas, Universidad Autónoma del Estado de Hidalgo, Mineral de la Reforma, Mexico
‡Centro de Investigaciones Químicas, Universidad Autónoma del Estado de Morelos, Cuernavaca, Mexico
§Facultad de Ciencias Químicas, Universidad de Colima, Colima, Mexico

(*Received 5 January 2014; accepted 23 April 2014*)

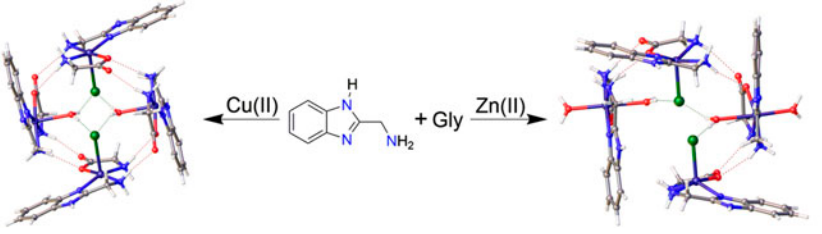

Reactions of 2-(aminomethyl)benzimidazole di-hydrochloride (**1**·2HCl) and glycine with 3Zn$(OH)_2$·2$ZnCO_3$ or Cu$(OAc)_2$·H_2O led to the synthesis of the quaternary coordination complexes **2** and **3**. X-ray diffraction showed that these complexes are composed of **2a** = [Zn(L)Cl(L′)] and **2b** = [Zn(L)$(H_2O)_2$(L′)], and of **3a** = [Cu(L)$(H_2O)_{0.25}$Cl(L′)] and **3b** = [Cu(L)$(H_2O)_{1.5}$(L′)], respectively, where L = 2-(aminomethyl)benzimidazole and L′ = glycinate. Zn(II) in **2a** has an intermediate geometry between a square-pyramid and a trigonal bipyramid structure. However, the geometry about the metal ion of units **2b**, **3a**, and **3b** is distorted octahedral. Moreover, the supramolecular structures for **2** and **3** were assembled through N–H···O and O–H···Cl hydrogen bonds. In these complexes, H_2O and N–H groups serve as proton donors, whereas chloride and C=O groups serve as proton acceptors. Also π–π stacking interactions between aromatic rings contribute to the stabilization of the supramolecular structure of **2** and **3**. The Zn and Cu complexes were studied by infrared and Raman spectroscopy, which indicated that **2** and **3** have similar molecular structures in the solid state. Ultrasound activation at the end of the reaction was necessary to yield **2**.

Keywords: Zinc; Copper; Hydrogen bonds; Ultrasound

1. Introduction

Zn(II) and Cu(II) are important in chemical and biological systems. Therefore, a wide variety of organic compounds have been used as ligands for Zn(II) and Cu(II) complexes [1, 2].

*Corresponding authors. Email: tlahuext@uaem.mx (H. Tlahuext); tapiab@uaeh.edu.mx (A.R. Tapia-Benavides)

© 2014 Taylor & Francis

Downloaded by [Institute Of Atmospheric Physics] at 15:14 09 December 2014

Complexes derived from imidazole, benzimidazole, and amino acid ligands are model compounds of particular bioinorganic interest [3, 4]. The imidazole moiety is essential in metalloproteins, and its interaction with Zn(II) and Cu(II) has profound effects on the biological actions of these macromolecules [5, 6]. In this context, 2-(aminomethyl)benzimidazole **1** is a very useful ligand in coordination chemistry because it can coordinate with transition metals such as V, Co, Ni, Pd, and Cd [7–10]. Thus, **1** has been used as a molecular model to explain the substrate–metal interactions in biochemical systems [7–10]. However, even though Zn and Cu are neighboring elements in the periodic table, these metals have different chemical behavior when interacting with 2-(aminomethyl)benzimidazole. Zn(II) coordinates with one or two **1** ligands as a function of pH and can assume diverse geometries in the solid state with different assemblies through N–H···Cl and O–H···Cl hydrogen bonds, whereas Cu(II) yields square-pyramidal or distorted octahedral complexes [11–13]. This behavior is chemically and biologically relevant, and for this reason, we are interested in the synthesis and structure of Zn(II) and Cu(II) complexes using **1** as a ligand.

Quaternary complexes of 2-(aminomethyl)benzimidazole and leucine or gly–gly dipeptide have been reported [14, 15]. However, a systematic study for the synthesis of Zn(II) or Cu(II) complexes derived from **1** and amino acids has not been reported. Aljahdali *et al.* proposed that the formation of **2** and **3** is thermodynamically viable in the presence of **1**, glycine, and the corresponding metal ion [figure 1(A)] [10, 16]. However, the formation of these complexes has not been demonstrated by spectroscopic and crystallographic methods. We believe that it is possible to promote the coordination of 2-(aminomethyl)benzimidazole, glycine, and X (Cl^- or H_2O groups) with metal by controlling the pH of the solution and the concentration of the chloride. In this article, we report on studies performed to identify the suitable reaction conditions for the synthesis of **2** and **3** in aqueous solution. The structural characterizations of **2** and **3** were performed by infrared (IR), Raman, and nuclear magnetic resonance (NMR) (only for **2**) spectroscopy; elemental and thermogravimetric analysis (TGA); and X-ray diffraction.

2. Experimental

2.1. *Materials*

Water was deionized prior to use. All reagents were purchased and used without purification. 2-(Aminomethyl)benzimidazole di-hydrochloride was synthesized as previously reported [17, 18].

2.2. *Physical and chemical measurements*

The ^1H and ^{13}C NMR spectra were recorded on a Varian 400 MHz spectrometer. The chemical shifts (δ ppm) are relative to the external reference CH_3OH ($\delta = 3.31$ for proton NMR and $\delta = 49.1$ for carbon NMR). IR and Raman spectra were recorded on a Perkin-Elmer System 200 FT-IR spectrophotometer. The elemental analyses were performed on a 2400 Perkin-Elmer Series II CHNS/O analyzer. The TGA studies were performed on a SDT Q 600 instrument. The melting points were measured on a Buchi Melting Point B-450 apparatus and were not corrected.

X-ray diffraction studies were performed on an Xcalibur Atlas Gemini diffractometer with a charge-coupled device area detector (λMoK$\alpha = 0.7107$ Å, monochromator: graphite). The

Downloaded by [Institute Of Atmospheric Physics] at 15:14 09 December 2014

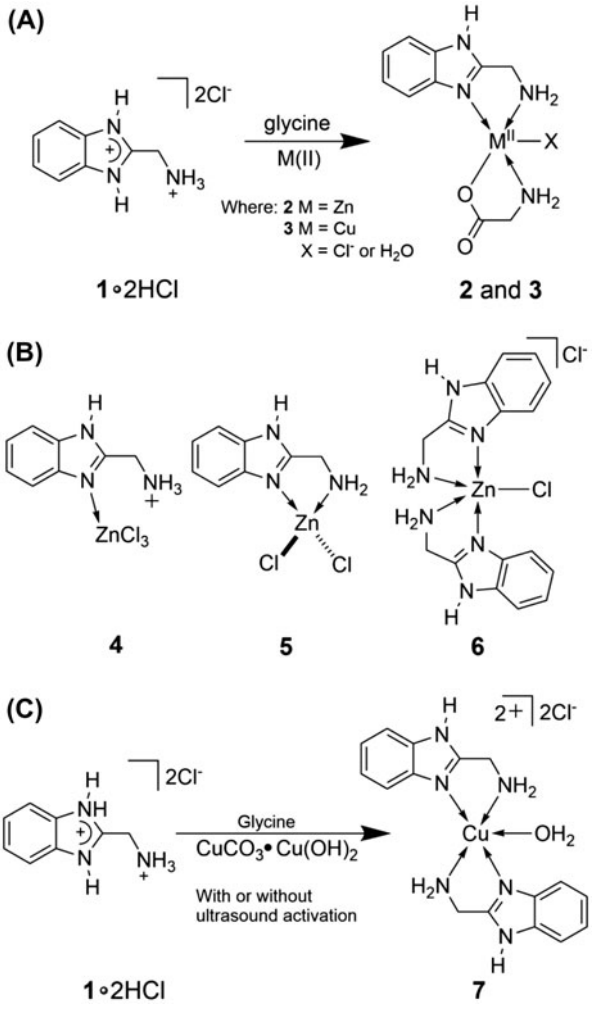

Figure 1. (A) Synthesis of **2** and **3** derived from 2-(aminomethyl) benzimidazole di-hydrochloride (**1**·2HCl), glycine, and metal ions. (B) Zn complexes **4**–**6** reported in Ref. [12]. (C) Reaction of di-hydrochloride of **1**, glycine, and $CuCO_3 \cdot Cu(OH)_2$ at different pH values, with or without ultrasound activation of the reaction.

frames were collected at $T = 301$ K (**2**) and $T = 296$ (**3**) via ω/ϕ-rotation at 10 s per frame. The measured intensities were corrected for absorption [empirical absorption correction using spherical harmonics, implemented with the SCALE3 ABSPACK scaling algorithm (CrysAlisPro, Agilent Technologies)] [19]. The structure solution, refinement, and data output were performed using the SHELXTL-NT program package [20]. The non-hydrogen atoms were anisotropically refined. The C–H hydrogens were placed in geometrically calculated positions using a riding model with $d(C–H_{aryl}) = 0.93$ Å and $U_{iso}(H_{aryl}) = 1.2\ U$eq (C). The hydrogens bonded to N (H1A, H1B, H3, H4A, H4B, H5A, H5B, H7, H8A, H8B) and O (H3A, H3B, H4C, H4D, H7B, H7C) were localized by difference Fourier maps. The coordinates of the N–H and O–H hydrogens were refined using the following constraints: $d(N–H) = 0.89(1)$ Å, $d(N–H_{imidazolic}) = 0.86(1)$, $d(O–H) = 0.82(1)$ Å, and

Downloaded by [Institute Of Atmospheric Physics] at 15:14 09 December 2014

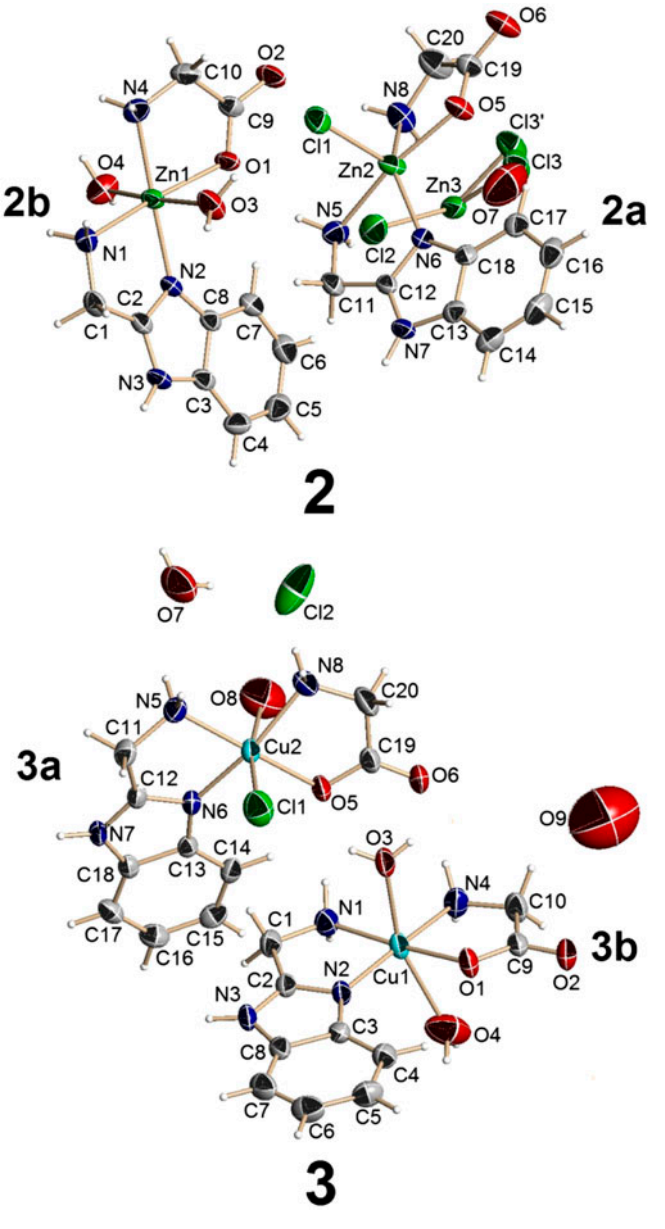

Figure 2. Molecular structures of **2** and **3** with atom labels and the local coordination geometries around Zn(II) and Cu(II). Thermal ellipsoids are shown at 50% probability level.

$U_{iso}(H) = 1.5\ U_{eq}(N,O)$. The networks contained one water for **2** (O7 refined occupancy 0.5) and two waters for **3** (disordered O8, O9 refined occupancies of 0.25), which are disordered around the crystallographic symmetry centers. Their hydrogens could not be located by difference Fourier maps. Figures 2–5 are drawn with DIAMOND [21] and OLEX 2 [22] using spheres of arbitrary radius.

Downloaded by [Institute Of Atmospheric Physics] at 15:14 09 December 2014

2.3. *Synthesis*

The syntheses of **2** and **3** were performed at controlled pH values. Moreover, strict control of the concentrations of the ligands and metal salts was important to obtain these complexes.

2.3.1. Complex 2. A mixture of 2-(aminomethyl)benzimidazole di-hydrochloride (117 mg, 0.533 mM) and glycine (60 mg, 0.800 mM) was dissolved in 5 mL of deionized water and activated with ultrasound for 10 min. Next, 280 mg (0.510 mM) of $3Zn(OH)_2{\cdot}2ZnCO_3$ was added, and the resulting mixture was treated with ultrasound for 5 min. The solution was adjusted to pH 6.3 with 1.00 M NaOH and subjected to ultrasound for an additional 20 min (final pH 6.0). After the reaction was completed, the mixture was filtered and the solution was slowly evaporated. The helix **2** was obtained as colorless crystals (32 mg, 8%). M.p.: 202.6 °C. Elemental analysis (found: C, 32.44; H, 4.21; N, 14.62; Calcd for $C_{40}H_{62}Cl_6N_{16}O_{13}Zn_5$: C, 31.72; H, 4.13, 14.80%). δ_H (400 MHz; D_2O; MeOH): 3.40 (2H, b, O=C–*CH*$_2$–NH_2), 4.23 (2H, s, Bz–*CH*$_2$–NH_2), 7.32 (2H, b, H5, and H6), 7.60 (2H, b, H4, and H7). δ_C (100 MHz; D_2O; MeOH): 36.5 (C1), 41.8 (C10), 112.7 (C4), 117.6 (C7), 123.7 (C5, C6), 134.6 (C3), 138.5 (C8), 155.7 (C2). IR (KBr): ν_{max} cm^{-1} 3384 ν(H–O), 3322 $\nu(NH_2)$, 3273 $\nu(NH_2)$, 1603 ν_a(COO), 1489 ν(CN), 1402 ν_s(COO), 1111 $\rho_t(NH_2)$, 1083 $\rho_w(NH_2)$, 844 $\rho_r(H_2O)$, 776 π(C–H), 763 π(C–H), 528 ν(Zn–O) or $\rho_w(H_2O)$, 604 $\delta(CO_2)$, 490 ν(Zn–N) Raman (neat): ν_{max} cm^{-1} 1597 ν_a(COO), 1403 ν_s(COO), 842 $\rho_r(H_2O)$, 491 ν(Zn–N), 283 ν(Zn–Cl).

2.3.2. Complex 3. A mixture of 2-(aminomethyl)benzimidazole di-hydrochloride (117 mg, 0.533 mM) and glycine (60 mg, 0.800 mM) was dissolved in 5.0 mL of deionized water and homogenized by ultrasound for 5 min. The resulting solution was added to $Cu(OAc)_2{\cdot}H_2O$ (107 mg, 0.533 mM) and shaken for 5 min. Next, the mixture was adjusted to pH 2.8 with 1.00 M NaOH and filtered. Complex **3** was obtained by slow evaporation of the aqueous solution as blue crystals (32 mg, 9%). M.p.: 183.4 °C. Elemental analysis (found: C, 34.24; H, 4.45; N, 15.30; Calcd for $C_{20}H_{32}Cl_2N_8O_7Cu_2$: C, 34.59; H, 4.64, 16.13%). IR (KBr): ν_{max} cm^{-1} 3398 ν(OH), 3321, $\nu(NH_2)$, 3272 $\nu(NH_2)$, 1602 ν_a(COO), 1492 ν(CN), 1401 ν_s(COO), 1118 $\rho_t(NH_2)$, 1051 $\rho_w(NH_2)$, 846 $\rho_r(H_2O)$, 782 π(C–H), 760 π(C–H), 672 ρ_r(Cu–H_2O) and ρ_r(Cu–NH_2), 543 ν(Cu–O) or $\rho_w(H_2O)$, 501 ν(Cu–N). Raman (neat): ν_{max} cm^{-1} 1592 ν_a(COO), 242 ν(Cu–Cl).

3. Results and discussion

3.1. *Synthetic procedures*

We performed the reaction of di-hydrochloride of **1**, glycine, and $ZnCl_2$ in aqueous solution at different pH values [from 2.4(1) to 5.4(1) at 0.5 intervals] in an attempt to produce **2**. The pH of the medium was fixed using NaOH, followed by slow evaporation. Nevertheless, **2** was not obtained under these reaction conditions. Instead of **2**, **4**–**6** were crystallized, depending on the working pH [figure 1(B)]. Compounds **4**–**6** have been reported [12]. These results should have been due to the presence of excess chloride in the reaction. To

maintain a constant chloride : benzimidazole proportion (2 : 1 equivalents), we used 3Zn $(OH)_2 \cdot 2ZnCO_3$; however, the quaternary complex was again not formed.

It is known that hydrogen interactions and crystallization are promoted by ultrasound treatment [23, 24]. Therefore, mixtures of **1**·2HCl, glycine, and $3Zn(OH)_2 \cdot 2ZnCO_3$ at different pH values [pH: 3.9(1), 5.0(1), 6.0(1), 6.3(1), and 7.0(1)] were activated using ultrasound (42 kHz and 100 W) at the end of the reaction. Complex **2** was only produced at pH of 5.0(1)–6.3(1) and **1**·2HCl : glycine : $3Zn(OH)_2 \cdot 2ZnCO_3$ molar ratios of 1 : 1.5 : 1.

Cu and Zn have different chemical and structural behaviors. For example, Zn(II) has a ligand-field stabilization energy of zero and can adopt diverse geometries. However, Cu complexes generally have square, square-pyramidal or distorted octahedral geometries [25]. Moreover, Cu complexes usually have higher stability constants and are predicted to be easier to synthesize than Zn complexes [10]. For this reason, we performed the reaction of the di-hydrochloride of **1** and glycine with $CuCO_3 \cdot Cu(OH)_2$. The process was performed at two different pH values [2.5(1) and 3.0(1)] with or without ultrasound activation. Nevertheless, the reaction preferentially yielded **7** [figure 1(C)]. Compound **7** has been reported [11, 18].

In view of the results obtained with $CuCO_3 \cdot Cu(OH)_2$, we chose to use $Cu(OAc)_2 \cdot H_2O$ because this salt is very soluble in aqueous solutions. Moreover, the acetate can be easily replaced and Cu(II) reactivity significantly increases. Again, we performed the reaction of the di-hydrochloride of **1** and glycine with $Cu(OAc)_2 \cdot H_2O$ at pH of 2.5(1), 2.8(1), and 3.3 (1) with or without ultrasound activation at the end of the reaction. In this case, the slow evaporation of the reaction yielded **3** as blue crystals. The best yield and best crystals were obtained at pH 2.8(1) without ultrasound activation and at molar ratios of 1 : 1.5 : 1.

3.2. *Crystallography*

Analysis by single-crystal X-ray diffraction showed that these complexes are assembled through N–H···O and O–H···Cl hydrogen bonds, producing helical supramolecular structures [with dissymmetric motifs (C_2)] for **2** and pseudo-tubular supramolecular structures for **3**. Both crystals are formed by crystallographically independent units with the general formula $\{[Zn^{II}(L)Cl(L')][Zn^{II}(L)(H_2O)_2(L')][0.5Zn^{II}Cl_4][0.5H_2O]\}_\infty$ for **2** and $\{[Cu^{II}(L)Cl(H_2O)_{0.25}(L')]\ [Cu^{II}(L)(H_2O)_{1.5}(L')][Cl][1.25H_2O]\}_\infty$ for **3** (L = 2-(aminomethyl)benzimidazole, L′ = glycinate). The molecular structures of the complexes are illustrated in figure 2. Crystal data and selected bond lengths, bond angles, and torsion angles are provided in tables 1 and 2, and the hydrogen bonding parameters are provided in table 3.

Complex **2** crystallizes in the monoclinic centrosymmetric space group *C2/c* and exhibits three crystallographically independent complex units: **2a** = [Zn(L)Cl(L′)]; **2b** = [Zn(L) $(H_2O)_2(L')$], [$0.5ZnCl_4$]; and a water molecule disordered around a crystallographic symmetry center (O7, refined occupancy 0.5). These results are in agreement with the elemental analysis and thermogravimetric studies, which corroborate the incidence of 2.5 water molecules in **2** and the presence of tetrachlorozincate. The Zn(II) ions have different coordination environments. **2a** is composed of 2-(aminomethyl)benzimidazole, glycinate, and Zn. The five coordination of the metal in **2a** is completed by a chloride. Consequently, the coordination geometry for Zn(II) is almost intermediate between a square-pyramid and a trigonal bipyramid ($\tau = 0.44$) [26].

In contrast to **2a**, the coordination environments for Zn(II) in **2b** have a distorted octahedral geometry whose equatorial plane is formed by 2-(aminomethyl)benzimidazole and

Downloaded by [Institute Of Atmospheric Physics] at 15:14 09 December 2014

Downloaded by [Institute Of Atmospheric Physics] at 15:14 09 December 2014

Table 1. Selected crystallographic and refinement data for **2** and **3**.

Complex	**2**	**3**
Empirical formula	$C_{40}H_{60}Cl_6N_{16}O_{13}Zn_5$	$C_{20}H_{32}Cl_2Cu_2N_8O_7$
Formula weight	1512.59	694.52
T (K)	301	296
λ (Å)	0.71073	0.71073
Crystal system	Monoclinic	Triclinic
Space group	*C2/c*	*P-1*
a (Å)	32.6958(16)	10.03735(17)
b (Å)	10.19457(16)	11.3306(2)
c (Å)	24.0068(11)	12.60323(19)
α (°)	90	90.6719(14)
β (°)	134.139(8)	105.6783(14)
γ (°)	90	97.0376(15)
V (Å^3)	5742.6(4)	1368.12(40)
Z	4	2
D_{Calcd} (mg mL^{-1})	1.750	1.686
Absorption coefficient (mm^{-1})	2.410	1.805
F (0 0 0)	3072.0	712.0
2θ (°)	6.48 to 50	5.94 to 51
Limiting indexes	$-38 \le h \le 38$, $-12 \le k \le 12$, $-28 \le l \le 28$	$-12 \le h \le 12$, $-13 \le k \le 13$, $-15 \le l \le 15$
Reflections collected	27,478	53,026
Independent reflections (R_{int})	5049(0.0398)	5093(0.0330)
Refinement method	Full-matrix least squares on F^2	Full-matrix least squares on F^2
Data/restraints/parameters	5049/16/426	5093/20/425
Goodness-of-fit (GOF) on F^2	1.026	1.026
Final R indexes [$I \ge 2s(I)$]	$R_1 = 0.0336$, $wR_2 = 0.0713$	$R_1 = 0.0290$, $wR_2 = 0.0724$
Final R indexes [all data]	$R_1 = 0.0482$, $wR_2 = 0.0772$	$R_1 = 0.0339$, $wR_2 = 0.0757$

Table 2. Selected bond lengths (Å), angles, and torsion angles (°) for **2** and **3**.

Complex **2**		Complex **3**	
N1–Zn1	2.135(3)	N1–Cu1	2.024(2)
N2–Zn1	2.066(3)	N2–Cu1	1.963(2)
N4–Zn1	2.103(3)	N4–Cu1	1.985(2)
O1–Zn1	2.074(2)	O1–Cu1	1.961(2)
O3–Zn1	2.285(2)	O3–Cu1	2.321(4)
O4–Zn1	2.128(2)	O4–Cu1	2.620(3)
N5–Zn2	2.189(3)	N5–Cu2	2.038(2)
N6–Zn2	2.039(3)	N6–Cu2	1.978(2)
N8–Zn2	2.067(3)	N8–Cu2	2.001(2)
O5–Zn2	2.086(2)	O5–Cu2	1.954(2)
O7–Zn2	3.14(3)	O8–Cu2	2.624(13)
Cl1–Zn2	2.346(1)	Cl1–Cu2	2.666(1)
N1–Zn1–N2	80.39(10)	N1–Cu1–N2	83.46(8)
N4–Zn1–O1	81.49(10)	N4–Cu1–O1	85.43(8)
O4–Zn1–O3	176.23(10)	O4–Cu1–O3	163.19(11)
N6–Zn2–N5	78.91(10)	N6–Cu2–N5	81.88(8)
N8–Zn2–O5	80.81(11)	N8–Cu2–O5	84.52(8)
N5–Zn2–Cl1	96.04(9)	N5–Cu2–Cl1	89.28(7)
O7–Zn2–Cl1	161.5(4)	O8–Cu2–Cl1	169.9(3)
N1–C1–C2–N2	2.9(4)	N1–C1–C2–N2	8.7(3)
N4–C10–C9–O1	−9.1(4)	N4–C10–C9–O1	−5.0(3)
N5–C11–C12–N6	12.0(4)	N5–C11–C12–N6	19.2(3)
N8–C20–C19–O5	−6.7(5)	N8–C20–C19–O5	−3.7(4)

Table 3. Hydrogen bond interactions (Å, °) for **2** and **3**.

D–H···A	D–H	H···A	D···A	D–H···A	Symmetry codes
Complex **2**					
N1–H1A···O5	0.88	2.17	3.027	162	$x, 1+y, z$
N1–H1B···Cl3	0.88	2.69	3.348	133	$x, 1-y, -1/2+z$
N3–H3···O2	0.86	1.91	2.746	162	$x, 1+y, z$
O3–H3A···Cl1	0.82	2.33	3.121	160	$½-x, ½+y, ½-z$
O3–H3B···Cl1	0.82	2.33	3.140	171	$x, 1+y, z$
N4–H4B···O6	0.89	2.12	3.006	176	$x, 1+y, z$
O4–H4C···Cl2	0.83	2.22	3.046	173	$-x, 1-y, -z$
O4–H4D···O2	0.82	1.93	2.746	170	$-x, 1-y, -z$
N5–H5A···O1	0.89	2.28	3.119	159	$½-x, -½+y, ½-z$
N5–H5B···Cl2	0.89	2.70	3.513	153	$½-x, -½+y, ½-z$
N7–H7···O6	0.86	1.92	2.761	166	$x, 1+y, z$
N8–H8A···Cl3	0.89	2.78	3.585	152	$½-x, -½+y, ½-z$
N8–H8A···O7	0.89	2.37	2.815	111	$½-x, -½+y, ½-z$
N8–H8B···O2	0.89	2.29	3.160	167	$½-x, -½+y, ½-z$
Complex **3**					
N1–H1B···Cl2	0.89	2.50	3.333	155	
N1–H1A···O5	0.89	2.14	3.029	176	
N3–H3···O2	0.86	1.90	2.740	166	$-1+x, y, z$
O3–H3A···Cl1	0.78	2.38	3.105	154	$1-x, -y, 1-z$
O3–H3B···Cl1	0.81	2.31	3.120	175	
N4–H4A···Cl2	0.89	2.83	3.604	146	
N4–H4B···O6	0.89	2.05	2.927	168	
O4–H4C···O7	0.83	2.19	2.899	144	$1-x, 1-y, -z$
O4–H4D···O2	0.83	2.08	2.889	165	$1-x, -y, -z$
N5–H5A···O2	0.89	2.10	2.976	172	$1-x, -y, 1-z$
N5–H5B···O7	0.89	2.32	3.150	157	$1-x, 1-y, 1-z$
N7–H7A···O6	0.86	1.90	2.741	165	$-1+x, y, z$
O7–H7B···Cl2	0.82	2.36	3.159	167	$1-x, 1-y, -z$
O7–H7C···Cl2	0.82	2.26	3.082	178	
N8–H8A···Cl2	0.89	2.69	3.500	152	$1-x, 1-y, 1-z$
N8–H8B···O1	0.89	2.23	3.117	175	$1-x, -y, 1-z$

Downloaded by [Institute Of Atmospheric Physics] at 15:14 09 December 2014

glycinate. The axial positions are occupied by two waters (O3, O4). The tetrachlorozincate (II) is situated on a crystallographic C_2 rotation axis with one of the chlorides disordered.

In contrast, **3** crystallizes in the triclinic centrosymmetric space group *P-1* (figure 2). The asymmetric unit comprises two crystallographically independent complex units, **3a** = [Cu(L)$(H_2O)_{0.25}$Cl(L′)] and **3b** = [Cu(L)$(H_2O)_{1.5}$(L′)] with one water disordered around crystallographic inversion symmetry centers (O9) (refined occupancies of 0.25); and a water molecule in a general position (O7). Again, the crystallographic results agree with the elemental analysis and TGA studies, which confirm the incidence of three water molecules in **3**. In **3a** and **3b**, Cu(II) ions have six-coordinate geometry. Thus, O8 is bonded to **3a** [Cu2–O8 bond length is 2.624(13) Å], but this oxygen is distorted and has an occupancy of 0.25. Moreover, the bond length Cu2–O8 and bond angle O8–Cu2–Cl1 [169.9(3)°] support the presence of a Jahn–Teller distortion in this unit [27, 28]. Otherwise, the Cu(II) in **3b** is embedded in a distorted six-coordinate geometry with Jahn–Teller distorted octahedral geometry, with one of the waters situated around a symmetry center (O3, refined occupancy 0.50).

The covalent M–O bonds are 2.074(2)–2.086(2) Å in **2** and 1.954(2)–1.961(2) Å in **3**. The covalent-coordinate M–N bond distances vary from 2.039(3) to 2.189(3) Å for **2** and from 1.963(2) to 2.038(2) Å for **3**, respectively. The covalent Zn–Cl and Cu–Cl bond distances are 2.346(1) and 2.666(1) Å, respectively. The covalent-coordinate M–O bond

distances (axial water molecules) are in the interval 2.128(2)–2.285(2) Å for **2** and 2.321 (4)–2.620(3) Å for **3**. The bond distances and angles within the ligands have characteristic values for Zn(II) and Cu(II) complexes [29, 30].

2a and **2b** are assembled through chains $C_2^1(4)$ involving [–O3–H3A···Cl1···H3B–] in disymmetric helical motifs, running along the *b* axis [table 3 and figure 3(A)] [31–33]. The

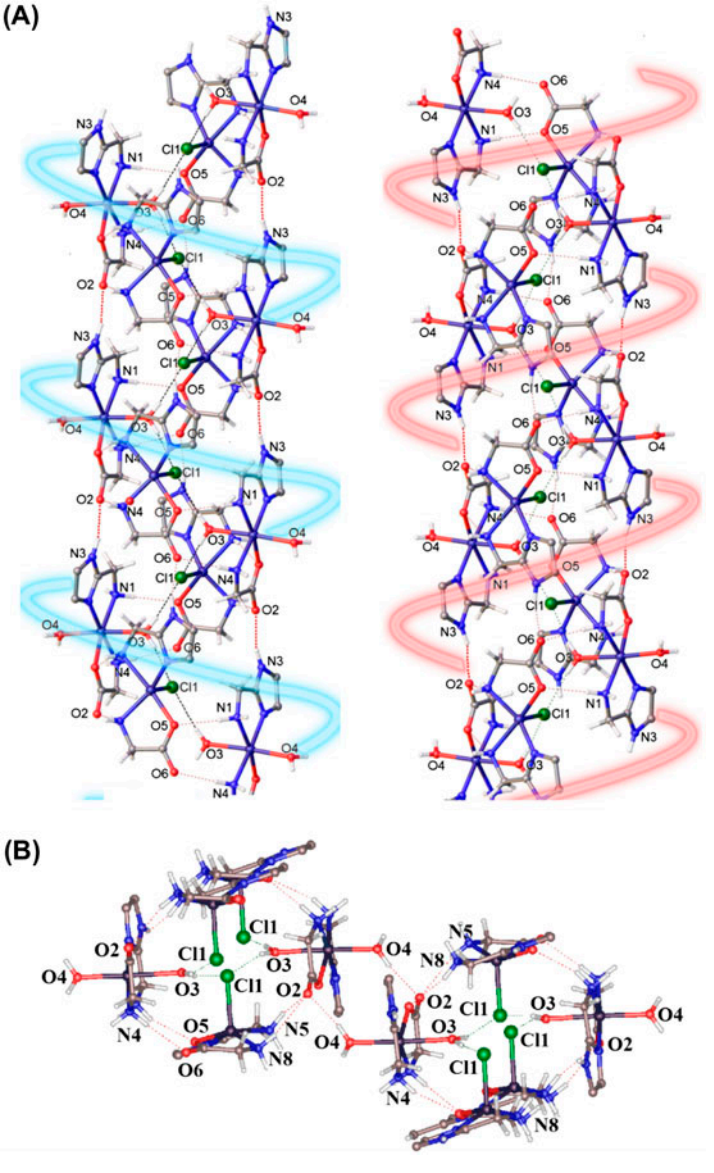

Figure 3. (A) View of the helical motif along the axis *b* for **2**, showing the N–H···O and O–H···Cl hydrogen bonds (dashed lines). Carbons and hydrogens of the benzimidazole moiety that are not involved in the hydrogen bonding interactions are omitted for clarity. (B) Pseudo-helical motifs connected by hydrogen bond interactions O4–H4D···O2.

Downloaded by [Institute Of Atmospheric Physics] at 15:14 09 December 2014

Downloaded by [Institute Of Atmospheric Physics] at 15:14 09 December 2014

O3···Cl1 lengths [3.121(2) and 3.140(2) Å] are shorter than the sum of their van der Waals radii [25]. Moreover, O3–H3A···Cl1 [160(5)°] and O3–H3B···Cl1 [171(5)°] bond angles are almost linear and indicate the presence of strong hydrogen bond interactions. Indeed, the presence of N–H···O hydrogen bond interactions contribute to the stabilization of the supramolecular structure. **2a** forms stable chains with graph set C(8) as well as **2b**. **2b** is brought together by N3–H3···O2 hydrogen bond interactions, whereas **2a** is united by N7–H7···O6 interactions. The interatomic lengths N···O [2.746(3) Å for **2b** and 2.761(4) Å for **2a**] and bond angles N–H···O [162(7)° for **2b** and 166(3)° for **2a**] show that these are strong hydrogen bond interactions. Moreover, the interaction between amine and carboxylate groups gives cyclic patterns $R_2^2(8)$ [–Zn2–N8–H8B···O2–C9–O1···H5A–N5–] that put together the **2a** and **2b** units. Moreover, these rings give a helical chain with graph set $C_2^2(8)$ [–N5–H5A···O1–Zn1–N1–H1A···O5–Zn2–] [figure 3(B)]. Therefore, the chain of rings yield a helical motif with graph set $C_2^2(8)R_2^2(8)$. However, *C2/c* is a centrosymmetric spatial group, and the crystalline structure is therefore formed by racemic mixtures of helical motifs [figure 3(A)]. Moreover, the water O4 has an important role in the formation of the crystal structure **2**. O4 is strongly coordinated to Zn1 [2.128(2) Å] and produces the six-coordination geometry of Zn in **2b**. Indeed, racemic helical motifs are connected by hydrogen bond interactions O4-H4D···O2 [O4···O2 length is 2.746(5) Å] and perhaps stabilizes the crystal structure of **2** [figure 3(B)].

In contrast, **3a** and **3b** have Jahn–Teller distortions and are assembled through O3–H3···Cl1 with a cyclic graph set $R_4^2(8)$ [–O3–H3B···Cl1···H3A–O3–H3B···Cl1···H3A–] producing pseudo-tubular structures running along the *a* axis [figure 4(A)]. The crystal structure of **3** has the spatial group *P-1*, and consequently, inversion centers are inside of the pseudo-tubular structures. Indeed, **3a** and **3b** are linked by N1–H1A···O5 [3.029(3) Å, 176(3)°], N4–H4B···O6 [2.927(3) Å, 168(3)°], N5–H5A···O2 [2.976(3) Å, 171.9(19)°], and N8–H8B···O1 [3.116(3) Å, 175(3)°] interactions [figure 4(B)]. But, unlike **2**, these interactions in **3** give two cyclic graph sets $R_2^2(8)$ [–C9–O1···H8B–N8–Cu2–N5–H5A···O2–] and $R_2^2(8)$ [–C19–O5···H1A–N1–Cu1–N4–H4B···O6–] that bring together two **3a** and two **3b**. Like **2**, in the supramolecular structure of **3**, the units **3a** and **3b** are bonded by hydrogen bond interactions between carboxylate and imidazole [N3–H3···O2 for **3b** and N7–H7···O6 for **3a**]. Thus, the interatomic lengths N···O [2.740(3) Å for **3b** and 2.741(3) Å for **3a**] and bond angles N–H···O [165.61(14)° for **3b** and 164.94(13)° for **3a**] show that these hydrogen bond interactions are strong and give chains with graph set C(8). In addition, the presence of distorted water O9 is important to stabilize the pseudo-tubular structure. Moreover, Jahn–Teller distorted O4→Cu bonds contribute to crystal lattice stabilization because pseudo-tubular structures are connected by O4–H4D···O2 interactions [figure 4(B)].

In both crystal structures for **2** and **3**, the motifs are associated through O–H···O hydrogen bonds to yield the graph sets $R_2^2(12)$, involving $(\cdots H4D–O4–M1–O1–C9–O2\cdots)_2$ (figures 4 and 5). In contrast, chlorides in tetrachlorozincate(II) [$ZnCl_4$] are acceptors of two H atoms (N1–H1B···Cl3···H8A–N8; N5–H5B···Cl2···H4C–O4) and interconnect four helices in **2** [figure 5(A)].

In contrast, in **3**, the water (O7) and the chloride Cl2 generate, through H–O–H···Cl hydrogen bonds, the centrosymmetric motif $R_4^2(8)$ $(\cdots Cl2\cdots H7B–O7–H7C\cdots)_2$, which interconnects four pseudo-tubular motifs through O–H···O, N–H···O, and N–H···Cl hydrogen bonds [figure 4(C) and table 3]. Moreover, the packing of the helical motifs in **2** and **3** is further stabilized by offset $\pi\cdots\pi$ interactions between adjacent complex units, with the following distances between the ring centroids: Cg1–Cg1 (3.590 for **2** and 3.732 Å for **3**) and Cg2–Cg3 (3.595 for **2** and 3.625 Å for **3**). Cg1 and Cg2 are the centroids of the imidazole

Downloaded by [Institute Of Atmospheric Physics] at 15:14 09 December 2014

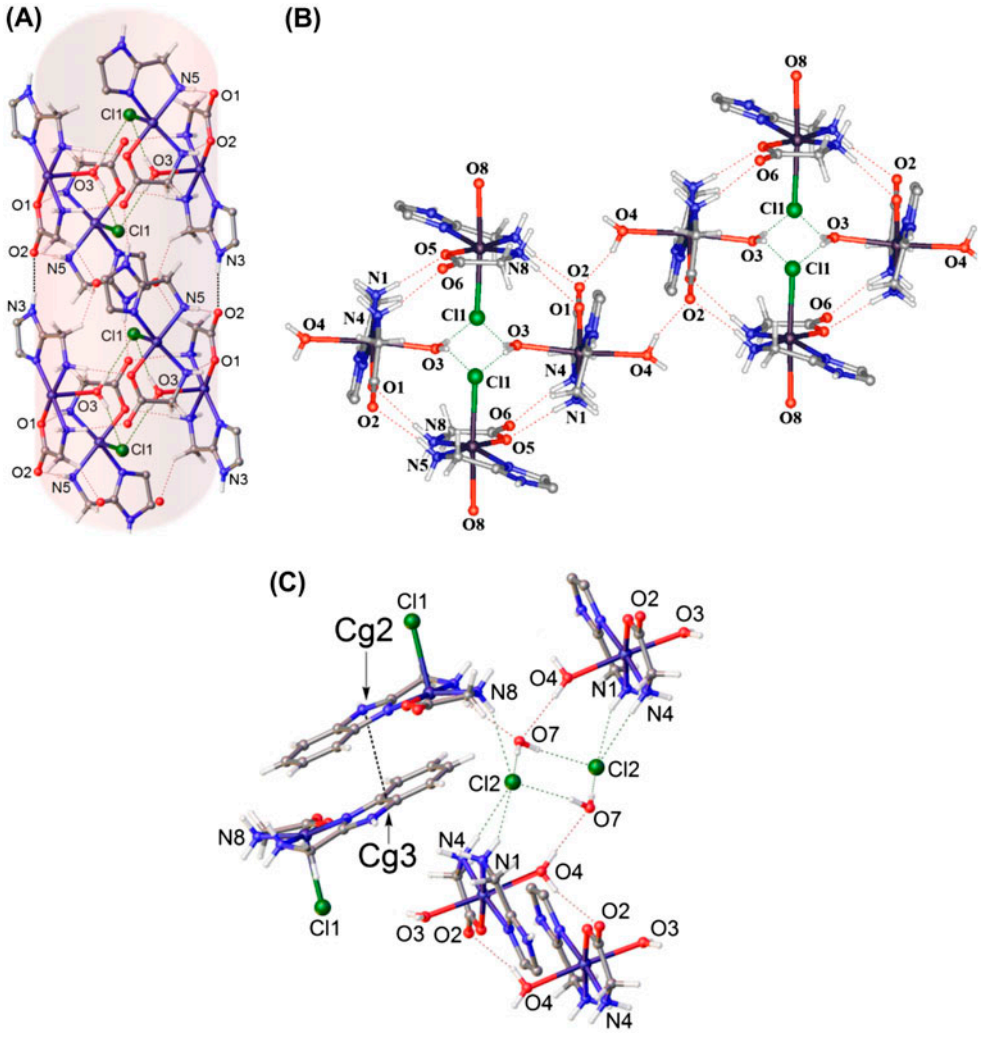

Figure 4. (A) Pseudo-tubular structure of **3**. (B) Pseudo-helical motifs are stabilized and connected by water molecules in Jahn–Teller distorted positions. (C) Pseudo-tubular structures in **3** are interconnected by graph set $R_4^2(8)$ $[Cl2\cdots H7C–O7–H7B\cdots]_2$, O4–H···O2, and Cg2–Cg3 π interactions. Carbons and hydrogens of the benzimidazole moiety that are not involved in hydrogen bonding interactions are omitted for clarity. Moreover, distorted water O9 is omitted for clarity.

rings N2/C2/N3/C3/C8 and N6/C12/N7/C13/C18, respectively, and Cg3 is the centroid of the benzene ring C13–C18 [figures 4(C) and 5(B)].

3.3. *Spectroscopic characterization*

The vibrational spectra of **2** and **3** are similar, which corroborates that both complexes have analogous molecular structures in the solid state. The IR spectra of **2** and **3** indicate the presence of water molecules with similar patterns of hydrogen bond interactions. In

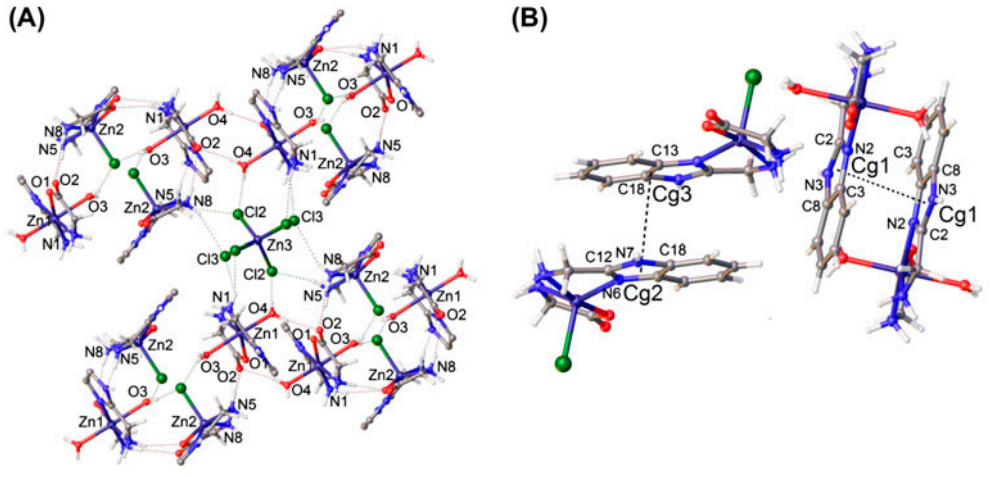

Figure 5. (A) Fragment of the supramolecular structure of **2**, showing the helices interconnected through O4–H···O2, O4–H···Cl2, N5–H···Cl2, and N8–H···Cl3 hydrogen bonds. (B) Cg1–Cg1 and Cg2–Cg3 π interactions in **2**.

both cases, the bands from 3600 to 2660 cm^{-1} are strong and broad, which suggest the presence of supramolecular hydrogen interactions in these complexes [15, 27, 34, 35]. The presence of water in these compounds is evidenced by $\rho_r(H_2O)$ vibrations at 844 cm^{-1} for **2** and 846 cm^{-1} for **3**, respectively. Whereas, the $\rho_w(H_2O)$ vibrations appear at 528 cm^{-1} for **2** and 543 cm^{-1} for **3** [36–38]. Indeed, the broad signal at 672 cm^{-1} suggests the presence of $H_2O\rightarrow Cu$ and $H_2N\rightarrow Cu$ coordinated bonds in **3** [35–38]. IR spectra of **2** and **3** have the characteristic of asymmetric (1603 cm^{-1} for **2** and 1602 cm^{-1} for **3**) and symmetric (1402 cm^{-1} for **2** and 1401 cm^{-1} for **3**) COO stretching frequencies. Separations between ν_a(COO) and ν_s(COO) vibrations (δ = 200 cm^{-1} for **2** and 191 cm^{-1} for **3**) show that carboxylates are unidentate bonded to metal ions in **2** and **3** [15, 38–40]. Broad signal at 543 cm^{-1} (for **3**) and 528 cm^{-1} (for **2**), previously assigned to $\rho_r(H_2O)$, could include the ν(M-O) vibrations [38]. Moreover, the signals at 490 cm^{-1} (for **2**) and 501 cm^{-1} (for **3**) were assigned to ν(M–N) vibrations and support the presence of chelate coordination in these complexes [12, 14, 41, 42]. On the other hand, unlike **1**·2HCl, C–H out plane bending (776 and 763 cm^{-1} for **2** and 782 and 760 cm^{-1} for **3**) are clearly different in chelate complexes derived from 2-(aminomethyl)benzimidazole [12]. Separation of these bands in Zn- and Cu-complexes (δ = 13 cm^{-1} for **2** and 22 cm^{-1} for **3**) corroborates the presence of chelate complexes.

Raman spectrum of **2** confirms that carboxylate groups are unidentate [ν_a(COO) = 1597 cm^{-1} and ν_s(COO) = 1403 cm^{-1}]. Likewise, the H_2O rocking vibration at 842 cm^{-1} was observed. The existence of Zn–N and Zn–Cl bonds was confirmed with absorptions at 491 and 283 cm^{-1}, respectively [43–46]. In contrast, the Raman spectrum of **3** showed the ν_a(COO) vibration at 1592 cm^{-1} and ν(Cu–Cl) at 242 cm^{-1}, respectively.

^1H and ^{13}C NMR spectra corroborated that **2** is present in aqueous solution. In the ^1H NMR spectrum, all resonances of **2** are shifted to low frequencies with respect to glycine and **1**·2HCl. These changes are more significant in methylene hydrogen nuclei ($\Delta\delta$ = 0.49 for H1 and 0.13 for H10) and can be explained by the inductive effect due to the presence of N→Zn coordination bonds.

Downloaded by [Institute Of Atmospheric Physics] at 15:14 09 December 2014

Downloaded by [Institute Of Atmospheric Physics] at 15:14 09 December 2014

The ^{13}C NMR spectrum of **2** has only one set of signals, and therefore, it is unlikely that a supramolecular structure exists in aqueous solution. The spectrum of **2** is asymmetric and all resonances of carbon nuclei are different. The presence of **2** with a quaternary structure is corroborated because there are chemical shifts to higher frequencies for C1–C3, C7–C8, and C10 ($\Delta\delta$ = 0.7–11.1). On the other hand, as in **4**–**6**, Zn complexes are characterized by bond-breaking phenomena (L→Zn ⇆ L + Zn) [12, 47–49]. The high coordinate flexibility of N→Zn bonds allows the occurrence of an intermolecular proton transfer mechanism of benzimidazole with D_2O. This increases the symmetry and broadening of NMR signals. Nevertheless, in **2**, the strong N→Zn coordination bond of imidazole nitrogen produces distinct aromatic signals of carbon nuclei. Whereas in **1**·2HCl, and **4**–**6**, the carbon nuclei next to imidazole nitrogen (pairs C3–C8 and C4–C7) have the same chemical shifts, the resonances of these carbon nuclei in **2** are different (δ = 134.6 for C3; 138.5 for C8; 112.7 for C4 and 117.6 for C7). Thus, it is probable that the presence of the glycinate, bonded to Zn(II), stabilizes the quaternary structure of **2**. Finally, when the deutered solvent was evaporated, IR spectroscopy again demonstrated the presence of **2** in the solid state.

4. Conclusion

Complexes **2** and **3** were only synthesized and crystallized when low-chloride concentrations and controlled pH [5.0(1)–6.3(1) for **2** and 2.8 for **3**] were used in the reaction of **1**·2HCl and glycine with the corresponding metal ion [Zn(II) or Cu(II)]. Ultrasound activation was necessary to achieve the synthesis of **2**. However, the use of bigger chloride concentrations yielded **4**–**6** [for Zn(II)] or **7** [for Cu(II)] under these reaction conditions. Moreover, in these complexes, the molecular self-assembly of the units "**a**" and "**b**" yielded helical motifs for **2** and pseudo-tubular structures for **3**. The supramolecular structures are modulated by N–H···O and O–H···Cl hydrogen bonding interactions. This result is relevant because we demonstrated that it is possible to promote the synthesis of coordination compounds with supramolecular structures by controlling the concentration of the reactants and pH. The formation of the coordination compounds based on benzimidazoles and amino acid derivatives is important as these compounds have notable chemical and physical behaviors [42, 50–55].

Supplementary material

The CCDC 934649 and CCDC 934650 files contain the supplementary crystallographic data for **2** and **3**. These data can be obtained free of charge from http://www.ccdc.cam.ac.uk/conts/retrieving.html or from the Cambridge Crystallographic Data Center, 12 Union Road, Cambridge CB2 1EZ, UK; Fax: +44 1223 336 033; Email: deposit@ccdc.cam.ac.uk.

Funding

This work was supported by CONACyT [SEP-2007-84453], Scholarship CONACyT [227964], and Red-PROMEP [2012].

Downloaded by [Institute Of Atmospheric Physics] at 15:14 09 December 2014

Supplemental data

Supplemental data for this article can be accessed here [http://dx.doi.org/10.1080/00958972.2014.930139].

References

[1] R. Mukherjee. *Comprehensive Coordination Chemistry II*, Vol. 6, Elsevier, Oxford (2003).
[2] S.J. Archibald. *Comprehensive Coordination Chemistry II*, Vol. 9, Elsevier, Oxford (2003).
[3] C. Santini, M. Pellei, V. Gandin, M. Pochia, F. Tisato, C. Marzano. *Chem. Rev.*, **114**, 815 (2014).
[4] V. Alterio, A. Di Fiore, K. D'Ambrosio, C.T. Supuran, G. De Simone. *Chem. Rev.*, **112**, 4421 (2012).
[5] V. Pelmenschikov, M.R. Blomberg, P.E.M. Siegbahn. *J. Biol. Inorg. Chem.*, **7**, 284 (2002).
[6] K. Hasegawa, T. Ono, T. Noguchi. *J. Phys. Chem. A*, **106**, 3377 (2002).
[7] M.R. Maurya, A. Kumar, M. Ebel, D. Rehder. *Inorg. Chem.*, **45**, 5924 (2006).
[8] A.A. El-Sherif. *J. Solution Chem.*, **39**, 1562 (2010).
[9] M. Aljahdali. *Spectrochim. Acta A*, **112**, 364 (2013).
[10] A.A. El-Sherif. *J. Solution Chem.*, **35**, 1287 (2006).
[11] H. Tlahuext, M. Tlahuextl, S. López-Gómez, A.R. Tapia-Benavides. *Acta Cryst.*, **E63**, 1263 (2007).
[12] A.R. Tapia-Benavides, M. Tlahuextl, H. Tlahuext, C. Galan-Vidal. *Arkivoc*, **v**, 172 (2008).
[13] Y. He, H.-Z. Kou, R.-J. Wang, Y. Li. *Transition Met. Chem.*, **28**, 464 (2003).
[14] G. Carpinteyro-López, J.L. Alcántara-Flores, D. Ramírez-Rosales, R. Escudero, B.M. Cabrera-Vivas, S. Bernès, R. Zamorano-Ulloa, Y. Reyes-Ortega. *Arkivoc*, **v**, 31 (2008).
[15] W.-L. Liu, Y. Zou, C.-L. Ni, Z.-P. Ni, Y.-Z. Li, Y.-G. Yao, Q.-J. Meng. *J. Coord. Chem.*, **57**, 899 (2004).
[16] M. Aljahdali, A.A. El-Sherif. *J. Solution Chem.*, **41**, 1759 (2012).
[17] L.A. Cescon, A.R. Day. *J. Org. Chem.*, **27**, 581 (1962).
[18] H.-Y. Wu, H. Li, B.-L. Zhu, S.-R. Wang, S.-M. Zhang, S.-H. Wu, W.-P. Huang. *Transition Met. Chem.*, **33**, 9 (2008).
[19] Agilent. *CrysAlis PRO*, Agilent Technologies, Yarnton (2011).
[20] (a) G.M. Sheldrick. *SHELX86, Program for Crystal Structure Solution*, University of Göttingen, Germany (1986); (b) Bruker Analytical X-ray Systems. *SHELXTL-NT (Versions 5.10 and 6.10)* (1999/2000).
[21] DIAMOND. *Visual Crystal Structure Information System (Version 3.1, CRYSTAL IMPACT, Postfach 1251, D-53002)*, Bonn (2006).
[22] O.V. Dolomanov, L.J. Bourhis, R.J. Gildea, J.A.K. Howard, H. Puschmann. *J. Appl. Crystallogr.*, **42**, 339 (2009).
[23] R.-Y. Wang, X.-Y. Liu, J.-L. Li. *Cryst. Growth Des.*, **9**, 3286 (2009).
[24] T.H. Ngo, H. Berndt, D. Lentz, H.-U. Reissig. *J. Org. Chem.*, **77**, 9676 (2012).
[25] J.E. Huheey, E.A. Keiter, R.L. Keiter. *Inorganic Chemistry: Principles of Structure and Reactivity*, Harper-Collins College Publishers, New York (1993).
[26] A.W. Addison, T.N. Rao, J. Reedijk, J. van Rijn, G.C. Verschoor. *Dalton Trans.*, 1349 (1984).
[27] P. Naumov, L. Pejov, G. Jovanovski, T. Stanfilov, M. Teseska, E. Stajanovska. *Cryst. Growth Des.*, **8**, 1319 (2008).
[28] C.J. Simmons, H. Stratemeier, M.A. Hitchman, M.J. Riley. *Inorg. Chem.*, **45**, 1021 (2006).
[29] F.H. Allen, O. Kennard, D.G. Watson, L. Brammer, A.G. Orpen, R. Taylor. *J. Chem. Soc., Perkin Trans. II*, S1 (1987).
[30] A.G. Orpen, L. Brammer, F.H. Allen, O. Kennard, D.G. Watson, R. Taylor. *J. Chem. Soc., Dalton Trans.*, S1 (1989).
[31] R. Mondal, T. Basu, D. Sadhukhan, T. Chattopadhyay, M.M. Bhunia. *Cryst. Growth Des.*, **9**, 1095 (2009).
[32] L. Brammer, E.A. Bruton, P. Sherwood. *Cryst. Growth Des.*, **1**, 277 (2001).
[33] G. Aullón, D. Bellamy, A.G. Orpen, L. Brammer, E.A. Bruton, A.G. Orpen. *Chem. Commun.*, 653 (1998).
[34] B. Morzyk-Ociepa, E. Różycka-Sokołowska, D. Michalska. *J. Mol. Struct.*, **1028**, 49 (2012).
[35] K. Helios, R. Wysokiński, A. Pietraszko, D. Michalska. *Vib. Spectro.*, **55**, 207 (2011).
[36] C. Espinoza, J. Szczepanski, M. Vala, N.C. Polfer. *J. Phys. Chem. A*, **114**, 5919 (2010).
[37] J.R. Roscioli, E.G. Diken, M.A. Johnson. *J. Phys. Chem. A*, **110**, 4943 (2006).
[38] K. Nakamoto. *Infrared and Raman Spectra of Inorganic and Coordination Compounds, Part B*, John Wiley and Sons, Inc., New York (1997).
[39] V. Rajalakshmi, V.R. Vijayaraghavan, B. Varghese, A. Raghavan. *Inorg. Chem.*, **47**, 5821 (2008).
[40] I.S. de la Cueva, A.G. Sicilia, J.M. González, E. Bugelia, A. Castiñeiras, J. Niclós-Gutiérrez. *React. Funct. Polym.*, **36**, 211 (1998).
[41] H. Temel, Ü. Çakir, B. Otludil, H.I. Uğraş. *Synth. React. Inorg. Met.-Org. Chem.*, **31**, 1323 (2001).
[42] S.L. Xiao, Y.Q. Zhao, C.H. He, G.H. Cui. *J. Coord. Chem.*, **66**, 89 (2013).
[43] T. Giannerini, C.A. Tellez, E. Hollauer. *Quím. Nova*, **27**, 206 (2004).
[44] P.R. Reddy, M. Radhika, P. Manjula. *J. Chem. Sci.*, **117**, 239 (2005).

[45] N.M. Aghatabay, A. Neshat, T. Karabiyik, M. Somer, D. Haciu, B. Dülger. *Eur. J. Med. Chem.*, **42**, 205 (2007).
[46] M. Andersson, J. Hedin, P. Johansson, J. Nordstöm, M. Nydén. *J. Phys. Chem. A*, **114**, 13146 (2010).
[47] Q. Wu, J.A. Lavigne, Y. Tao, M. D'Iorio, S. Wang. *Inorg. Chem.*, **39**, 5248 (2000).
[48] H. Vahrenkamp. *Acc. Chem. Res.*, **32**, 589 (1999).
[49] M.A. Zoroddu, S. Medici, M. Peana, R. Anedda. *Dalton Trans.*, 1282 (2010).
[50] B. Liu, D. Zhao, T. Li, X.-R. Meng. *J. Coord. Chem.*, **66**, 139 (2013).
[51] H.-W. Kuai, T.-A. Okamura, W.-Y. Sun. *J. Coord. Chem.*, **65**, 3147 (2012).
[52] H.-W. Kuai, X.-C. Cheng, X.-H. Zhu. *J. Coord. Chem.*, **66**, 28 (2013).
[53] S.-X. Yan, D. Zhao, T. Li, R. Wang, X.-R. Meng. *J. Coord. Chem.*, **65**, 945 (2012).
[54] J.-C. Jin, W.-Q. Tong, C.-G. Xie, W.-G. Chang, G.-N. Xu, J. Wu, L.-G. Li, Z.-Q. Yan, Y.-Y. Wang. *J. Coord. Chem.*, **66**, 3697 (2013).
[55] J. Xu, X. Sun, C. Ju, J. Sheng, F. Wang, M. Sun. *J. Coord. Chem.*, **66**, 2541 (2013).

Downloaded by [Institute Of Atmospheric Physics] at 15:14 09 December 2014